Prediction of the Potential Distribution of Tirpitzia sinensis in China Based on the MaxEnt Model

Yaling Mao
Guizhou Normal University
Xiaoxin Tang
3653972450@qq.com
Guizhou Normal University
Wei Shi
Guizhou Normal University
Chao Zhang
Guizhou Normal University
Rundi Zhou
Guizhou Normal University

Research Article

Keywords: Tirpitzia sinensis, Maximum Entropy Model, Potential Distribution Area, Climate Change, Environmental Factors

Posted Date: June 25th, 2025

DOI: https://doi.org/10.21203/rs.3.rs-6863150/v1

Additional Declarations: No competing interests reported.

Version of Record: A version of this preprint was published at Environmental Monitoring and Assessment on September 15th, 2025. See the published version at https://doi.org/10.1007/s10661-025-14604-3.

Abstract

Tirpitzia sinensis, a traditional medicinal plant, is known for its ability to promote blood circulation, reduce swelling, alleviate pain, and assist in bone healing through its stems and leaves. This study utilized 174 valid distribution records of *Tirpitzia. sinensis* in China, along with 10 environmental variables, to predict its current and future distribution patterns. Using the MaxEnt model and ArcGIS software, the study also identified the climatic factors limiting its distribution. The results are as follows: (1) The MaxEnt model demonstrated extremely high predictive accuracy, with an Area Under the Curve (AUC) value of 0.985. Currently, the total suitable area for *Tirpitzia sinensis* covers 1,869,438 km², accounting for 19.47% of China's land area. This area is mainly concentrated in western Guangxi Province, southeastern Yunnan Province, southern Guizhou Province, southeastern Sichuan Province, and southwestern Chongqing Municipality. (2) The primary environmental factors influencing the potential distribution of *Tirpitzia sinensis* include precipitation during the warmest quarter (bio18), minimum temperature of the coldest month (bio06), temperature seasonality (bio04), and mean temperature of the driest quarter (bio09). (3) Under future climate change scenarios, the potential distribution area of *Tirpitzia sinensis* is expected to expand compared to the current distribution, with an overall trend of northward migration. Specifically, under the SSP126 climate scenario, the distribution center is projected to shift from Guizhou Province to Hunan Province. Under the SSP585 climate scenario, this shift extends further towards Hunan and Hubei Provinces.

Introduction

In the field of global change and biogeography research, the response of vegetation to climate change has always been a core focus (Bellard et al., 2012). Climate, as a key environmental factor influencing species and vegetation distribution at both regional and global scales, has profound and far-reaching effects on biodiversity and species range (Hamann & Wang, 2006). Future climate change may lead to changes in the distribution and abundance of species (Ehrlén & Morris, 2015), the extinction of species populations (Bestion et al., 2015), alterations in distribution ranges (Chen et al., 2011), phenological changes (Merilä & Hendry, 2014), as well as changes in physiological characteristics (Dillon et al., 2010). Exploring the trends in potential geographic distribution of species under future climate change scenarios and analyzing their response mechanisms are of irreplaceable importance for developing scientifically sound biodiversity conservation strategies. Furthermore, a comprehensive assessment of the impacts of climate change on species distribution can provide strong support for policymakers, enabling them to effectively address challenges arising from shifts in species ranges. This, in turn, helps maintain the stability of ecosystems and ensures the sustainable development of biodiversity (Zhang et al., 2018).

Climate is one of the main determinants delimiting geographical distribution of plant species on large scale. There is a considerable amount of research declaring climate change lead to the range expansion or retraction in plant species ranges. To assess the vulnerability of plant species under a rapidly changing climate, we can use species distribution modelling (SDM) to predict species climate niches and project their potential future range shifts (Thuiller et al., 2005). Currently, various SDMs are widely applied, including the Maximum Entropy Model (MaxEnt), Random Forest (RF), Boosted Regression Trees (BRT), Generalized Linear Models (GLM), and CLIMEX (CL) (Duan et al., 2014). Among them, the MaxEnt model, based on the principle of maximum entropy, has gained significant attention from researchers due to its superior accuracy, reproducibility, ease of operation, and low computational resource requirements. The MaxEnt model is a widely used species distribution modeling method in the fields of ecology and biogeography. By analyzing the relationship between known species distribution points and environmental variables, it effectively predicts the potential distribution areas of species. This is highly significant for assessing species' suitable habitats and ecological niches. Additionally, it identifies key environmental factors influencing species distribution, providing insights into their ecological requirements and adaptive mechanisms (Cao et al., 2022). In recent years, the MaxEnt model has been extensively applied in predicting the potential distribution of flora and fauna, as well as in habitat conservation. For instance, Chen Haojie et al. (Chen et al., 2021) used this model to analyze the potential distribution of *Populus euphratica* in China under future climate change scenarios; Liu Hua et al. (Liu et al., 2023) studied the potential distribution of *Liriodendron chinense*; and Gu Yuanyang et al. (Gu et al., 2020) predicted the potential habitat of the *Panthera tigris*, integrating the results with cost-distance methods to refine natural reserve planning within its habitat range.

Tirpitzia sinensis, belonging to the Linaceae family and the genus *Tirpitzia*, is a heterostylous plant that typically grows as a shrub or small tree. It thrives at elevations of 300–2400 meters, often on slopes and limestone substrates. The species is primarily distributed in the southwestern regions of China, including Guangxi, Guizhou, southeastern Yunnan, Hunan, and Chongqing, with occasional records in Vietnam. As a medicinal plant, *Tirpitzia sinensis* is valued for its stems and leaves, which possess properties for promoting blood circulation, reducing swelling, relieving pain, and facilitating bone healing (Du et al., 2014). Gu Ronghui et al. (Gu, 2015) conducted research on the chemical composition of *Tirpitzia sinensis* and discovered adenosine (5, Adenosine, TS-28), isolated from the plant for the first time. Adenosine is an extracellular signaling molecule that plays a critical role in human physiological activities. Its functions include inducing vasodilation, regulating blood pressure and heart rate, modulating the sympathetic nervous system, and exhibiting antithrombotic activity. By utilizing DS for reverse target screening of new compounds, the study speculated that Compound 2 is related to wound healing, Compound 3 is associated with inflammatory responses and cancer, and Compound 4 may have relevance to inflammation, aging processes, and wound healing.

This study, based on specimen distribution records and environmental data for *Tirpitzia sinensis* in China, simulated the plant's potential distribution under current climatic conditions. It conducted an in-depth analysis of the key environmental factors influencing plant distribution and identified the environmental range suitable for plant growth. Additionally, the study selected two climate scenarios, SSP126 and SSP585, for the time periods 2021–2040, 2041–2060, 2061–2080 and 2081–2100, to analyze changes in the geographic distribution of *Tirpitzia sinensis* and the shift in its geometric center under future climatic conditions. By clarifying the impact of climate change on the potential distribution of *Tirpitzia sinensis*, this study provides a scientific basis for the conservation of its population resources, the selection of artificial cultivation areas, and ecosystem management. Furthermore, given the significant medicinal value of *Tirpitzia sinensis*, the findings also hold vital importance for ensuring the sustainable use of its germplasm resources. In the future, as climate change intensifies, similar predictive studies will offer valuable references for the conservation and management of other important species.

Materials and methods

Collection and screening of distribution data

The distribution data of *Tirpitzia sinensis* were obtained from three main sources: Field sampling: Latitude and longitude coordinates were recorded using GPS during field surveys. Literature review: Relevant publications were reviewed to extract provided latitude and longitude data, or geographic coordinates were identified based on known place names (Huang et al., 2019). Online platforms: Distribution data, including latitude and longitude, were retrieved from various platforms such as the Chinese Virtual Herbarium (CVH, https://www.cvh.ac.cn/), the Global Biodiversity Information Facility (GBIF, https://www.gbif.org/), and the Plant Photo Bank of China (PPBC, http://ppbc.iplant.cn/). For records or specimens that lacked direct latitude and longitude information but included specific location details, coordinates were determined using Baidu Maps' coordinate picker tool. To ensure the accuracy of the predictive model and avoid clustering of multiple data points within the same area, distribution data were filtered using ENMtools at a spatial resolution of 2.5' (approximately 5 km) from the WorldClim Global Climate Database (http://www.worldclim.org) (Warren et al., 2010).Retain only one point per grid cell to reduce sampling bias in species distribution data. Ultimately, a total of 174 distribution records for *Tirpitzia sinensis* were obtained (Fig. 1).

Acquisition and processing of climate data

The current climate data (1970–2000) and future climate data (2021–2040, 2041–2060, 2061–2080, 2081–2100) used in this study were downloaded from the WorldClim Global Climate Database (https://www.worldclim.org/). These data include 19 climate variables related to temperature and precipitation, as well as elevation data, all with a spatial resolution of 2.5' (Fritz et al., 2017). Future climate data were selected from the Coupled Model Inter-comparison Project Phase 6 (CMIP6) and utilized the Beijing Climate Center Climate System Model 2 Medium Resolution (BCC-CSM2-MR), which is suitable for China's geographic environment. Two Shared Socioeconomic Pathways (SSPs) were considered: SSP126 and SSP585. SSP126 represents a sustainable development pathway aimed at limiting global warming to below 2°C, while SSP585 represents a business-as-usual pathway with projected warming of 3.3–5.7°C (Riahi et al., 2017). Slope and aspect data used in the study were extracted from DEM (Digital Elevation Model) elevation data, which were obtained from the Computer Network Information Center of the Chinese Academy of Sciences and the International Scientific Data Service Platform (http://www.gscloud.cn/) (Bi et al., 2005). The downloaded climate raster data (.tif) were converted into the (.asc) format compatible with the MaxEnt model using ArcGIS software.

Through pre-experimental runs of the MaxEnt model, the contribution percentage and permutation importance of the environmental factors were obtained, and factors with a contribution rate of 0 were excluded. Subsequently, Spearman correlation analysis was performed on 22 environmental variables using the ENMTools tool. Due to collinearity among variables, which could lead to overfitting of the distribution prediction model, variables with a correlation coefficient $|r| \geq 0.8$ were prioritized for exclusion, giving preference to removing those with lower contribution rates (Gao et al., 2023). Based on the contribution rate results from the MaxEnt model and the correlation analysis (Fig. 2), a total of 10 key environmental factors were ultimately selected (Table.1).

Table.1 The environmental variables used for the MaxEnt Model

Variable code	Variable type	Unit
bio01	Annual mean temperature	℃
bio04	Temperature seasonality	℃
bio06	Min temperature of coldest month	℃
bio09	Mean temperature of driest quarter	℃
biol1	Mean temperature of coldest quarter	℃
bio14	Precipitation of driest month	mm
bio18	Precipitation of warmest quarter	mm
aspect	Aspect	°
slope	Slope	°
elev	Elevation	m

Construction and Parameter Optimization of the MaxEnt Model

In this study, the Kuenm R package was used to optimize two parameters, namely Feature Combination (FC) and Regularization Multiplier (RM). By setting the range of the RM value from 0 to 4 with an interval of 0.5 and performing cross-combinations with five types of feature combinations, including Linear (L), Quadratic (Q), Product (P), Threshold (T), and Hinge (H), a total of 238 candidate models can be evaluated. Finally, the parameter combination with an omission rate of less than 5% and the minimum natural logarithm value of AICc was selected. That is, when the delta AICc value is 0, the corresponding FC and RM combination is the optimal one (Cobos et al., 2019).

Import 174 distribution data points and the selected 10 environmental factors into the MaxEnt 3.4.4 software to construct a species distribution prediction model. The model parameters are set as follows: First, the data is randomly divided into a training set and a testing set, with 75% of the distribution points used to train the model and 25% used to test the model's accuracy. To ensure the model's stability and result reproducibility, the analysis is run 10 times with repetitions, while other parameters are kept at the default settings of the MaxEnt software. The average value of the results is taken as the final output, and the output format is set to logistic for logical output representation (Zhao et al., 2021).

To evaluate the accuracy of the model's prediction results, the Receiver Operating Characteristic Curve (ROC) was employed, with the Area Under the ROC Curve (AUC) used as the evaluation metric (Cao, 2010). The AUC value reflects the reliability of the model's predictions and ranges from 0 to 1. Generally, the closer the AUC value is to 1, the better the model's predictive performance. Specifically, if the AUC value is less than 0.7, the model's predictive performance is poor; when the AUC value is between 0.7 and 0.8, the prediction results are at an average level; an AUC value between 0.8 and 0.9 indicates good predictive ability; and when the AUC value exceeds 0.9, the model's predictions are excellent and highly reliable (Li et al., 2023).

Suitability zone classification

Import the ASC format result files output by the MaxEnt model into ArcMap and use the Spatial Analyst toolbox for further analysis. Apply the Reclassify tool and use the natural breaks classification method in ArcMap to divide the potential suitable zones of *Tirpitzia sinensis* into four levels: non-suitable zone, low suitability zone, medium suitability zone, and high suitability zone. The suitability index levels are classified as follows: 0–0.1 (non-suitable zone), 0.1–0.3 (low suitability zone), 0.3–0.5 (medium suitability zone), and 0.5–1 (high suitability zone) (Zheng et al., 2024). Subsequently, calculate the proportion of each suitability level and determine the area size of each suitability level.

Changes in suitability zone patterns and centroid shifts

Using ArcMap software, the suitable habitat zones of *Tirpitzia sinensis* were divided into suitable and non-suitable zones based on the suitability index classification from the previous step. Using the SDMToolbox toolkit in ArcMap, the data from the earlier period was set as the current data, and the data from the later period was set as the future data. The changes in suitable zones between consecutive periods were categorized into non-suitable zones, expansion zones, contraction zones, and stable zones (Li et al., 2021). In ArcMap, the suitable zone maps under contemporary and future climate scenarios (SSP126 and SSP585) were overlaid, and the SDMToolbox toolkit was applied to calculate the vector centroids of the suitable zones (Jia et al., 2024). By analyzing the shifts in vector centroids under different climate conditions, the distribution trends of suitable zones for *Tirpitzia sinensis* were revealed, providing insights into the spatial pattern changes of its suitable distribution areas under contemporary and future climate scenarios.

Results and analysis

Evaluation of MaxEnt model accuracy

After running the MaxEnt model ten times, both the training and test set AUC values reached 0.985 (Fig. 3). This result clearly demonstrates the model's exceptionally high accuracy, meeting an excellent standard. Therefore, it can be reliably used to predict the suitable zones for *Tirpitzia sinensis.*

Major environmental factors influencing the geographical distribution of *Tirpitzia sinensis*

This study identified the major environmental factors influencing the geographical distribution of *Tirpitzia sinensis* based on the regularized training gain of 10 environmental variables in the MaxEnt model, as well as their percent contribution and permutation importance. Table 2 shows that the precipitation of the warmest quarter (bio18), minimum temperature of the coldest month (bio06), temperature seasonality (bio04), and elevation (elev) are key environmental factors. Among them, bio18 had the highest percent contribution, reaching 57.8%, followed by bio06 (18.9%), bio4 (10%), and elevation (3.4%). In terms of permutation importance, bio06 had the greatest impact at 71.3%, while bio18 was 3.3%, and bio04 and elevation contributed relatively less, at 1.7% and 1.5%, respectively. Figure 4 reveals that different environmental factors have varying degrees of influence on the distribution of *Tirpitzia sinensis*. The mean temperature of the driest quarter (bio09) showed the highest regularized training gain (2.37), followed by bio18, bio11, bio01, bio06 and bio04, with training gains of 1.96, 1.88, 1.83, 1.72, and 1.49, respectively. By combining the percent contribution and jackknife test results, the main environmental factors influencing the geographical distribution of *Tirpitzia sinensis* are bio18, bio06, bio04, and bio09.

Table.2 Percent contribution and permutation importance of environmental variables

Variable code	Variable type	Percent contribution(%)	Permutation importance(%)
bio18	Precipitation of warmest quarter	57.8	3.3
bio06	Min temperature of coldest month	18.9	71.3
bio04	Temperature seasonality	10	1.7
elev	Elevation	3.4	1.5
biol1	Mean temperature of coldest quarter	3.3	2.3
bio14	Precipitation of driest month	2.5	0.7
bio01	Annual mean temperature	1.4	0.7
bio09	Mean temperature of driest quarter	1.2	17.9
aspect	Aspect	0.9	0.4
slope	Slope	0.6	0.4

Response curves of environmental factors

A detailed analysis was conducted on the four main environmental factors influencing the distribution of *Tirpitzia sinensis*. The response curves of these factors to the presence probability of *Tirpitzia sinensis* are shown in Fig. 5.It is generally considered that when the presence probability exceeds 0.5, the corresponding range of environmental factors is suitable for the growth of *Tirpitzia sinensis*. As shown in Fig. 5, the presence probability of *Tirpitzia sinensis* exhibits an increasing and then decreasing trend with the increase in the four environmental factors: bio18, bio06, bio04 and bio09. bio18: The suitable range for growth is 582.4–907.1 mm. The presence probability reaches its maximum value of 0.67 when the precipitation is 656.7 mm, indicating that *Tirpitzia sinensis* prefers relatively drier areas. bio06: The suitable range is 2.6–8.1°C. The presence probability peaks at 0.70 when the temperature is 5.4°C. bio04: The suitable range is 432.9–712.8, with the presence probability reaching a maximum value of 0.66 when the standard deviation is 513.3. bio09: The suitable range is 7.7–14.1°C. The presence probability is highest at 0.73 when the temperature is 11.7°C.

Changes in suitability levels of *Tirpitzia sinensis*

Using MaxEnt modeling, the distribution of *Tirpitzia sinensis* was divided into four suitability levels: non-suitable, low suitability, medium suitability, and high suitability zones. Under current climatic conditions, the total suitable area for *Tirpitzia sinensis* is 1,869,438 km², accounting for 19.47% of China's total area. Among these: The high suitability zone covers 355,195 km², making up 3.70% of China's total area. These regions are mainly concentrated in the western part of Guangxi Zhuang Autonomous Region, southeastern Yunnan Province, southern Guizhou Province, southeastern Sichuan Province, and southwestern Chongqing Municipality. The medium suitability zone spans 633,774 km², representing 6.60% of China's total area. The low suitability zone extends over 880,469 km², accounting for 9.17% of China's total area.

Under the SSP126 climate scenario, from 2021 to 2040, the total suitable area for *Tirpitzia sinensis* is 2,027,673 km², accounting for 21.12% of China's total area. Among these, the high suitability zone covers 451,974 km² (4.71%), mainly concentrated in western Guangxi Zhuang Autonomous Region, southeastern Yunnan Province, Guizhou Province, southeastern Sichuan Province, Chongqing Municipality, and northwestern Hunan Province; the medium suitability zone spans 755,489 km² (7.87%); and the low suitability zone covers 820,211 km² (8.54%). Between 2041 and 2060, the total suitable area increases to 2,052,349 km², accounting for 21.38% of China's total area. The high suitability zone expands to 533,661 km² (5.56%), distributed in northern Guangxi Zhuang Autonomous Region, southeastern Yunnan Province, Guizhou Province, southeastern Sichuan Province, Chongqing Municipality, and western Hunan Province. The medium suitability zone is 728,764 km² (7.59%), and the low suitability zone is 789,925 km² (8.23%). From 2061 to 2080, the total suitable area slightly decreases to 1,986,812 km², accounting for 20.70% of China's total area. The high suitability zone increases to 592,687 km² (6.17%), mainly located in northern Guangxi Zhuang Autonomous Region, southeastern Yunnan Province, Guizhou Province, eastern Sichuan Province, Chongqing Municipality, northwestern

Hunan Province, southwestern Hubei Province, and northern Guangdong Province. The medium suitability zone shrinks to 633,973 km² (6.92%), and the low suitability zone is 730,153 km² (7.61%). Between 2081 and 2100, the total suitable area decreases further to 1,965,383 km², accounting for 20.47% of China's total area. The high suitability zone reduces to 492,783 km² (5.13%), mainly distributed in northern Guangxi Zhuang Autonomous Region, southeastern Yunnan Province, Guizhou Province, eastern Sichuan Province, Chongqing Municipality, northwestern Hunan Province, and southwestern Hubei Province. The medium suitability zone shrinks to 600,519 km² (6.26%), and the low suitability zone increases to 872,082 km² (9.08%).

Under the SSP585 climate scenario, from 2021 to 2040, the total suitable area for *Tirpitzia sinensis* is 1,979,623 km², accounting for 20.62% of China's total area. Among these, the high suitability zone covers 416,739 km² (4.34%), mainly concentrated in northern Guangxi Zhuang Autonomous Region, southeastern Yunnan Province, Guizhou Province, eastern Sichuan Province, and western Chongqing Municipality. The medium suitability zone spans 630,040 km² (6.56%), while the low suitability zone covers 932,844 km² (9.72%). From 2041 to 2060, the total suitable area increases to 2,114,849 km², accounting for 22.03% of China's total area. The high suitability zone expands to 495,648 km² (5.16%), mainly distributed in northern Guangxi Zhuang Autonomous Region, southeastern Yunnan Province, Guizhou Province, eastern Sichuan Province, Chongqing Municipality, northwestern Hunan Province, and southwestern Hubei Province. The medium suitability zone is 653,050 km² (6.80%), and the low suitability zone is 966,151 km² (10.06%). From 2061 to 2080, the total suitable area increases further to 2,344,282 km², accounting for 24.42% of China's total area. The high suitability zone reaches 679,341 km² (7.08%), mainly located in northwestern Guangxi Zhuang Autonomous Region, southeastern Yunnan Province, Guizhou Province, eastern Sichuan Province, Chongqing Municipality, northwestern Hunan Province, and southwestern Hubei Province. The medium suitability zone is 672,221 km² (7.00%), and the low suitability zone covers 992,720 km² (10.34%). From 2081 to 2100, the total suitable area decreases slightly to 2,201,694 km², accounting for 29.93% of China's total area. The high suitability zone reduces to 542,744 km² (5.65%), mainly distributed in Guizhou Province, eastern Sichuan Province, Chongqing Municipality, northwestern Hunan Province, western Hubei Province, and southern Shaanxi Province. The medium suitability zone shrinks to 535,103 km² (5.57%), while the low suitability zone expands to 1,123,848 km² (11.71%) (Figs. 6, 7 and 8).

Changes in suitable areas and centroid shifts of *Tirpitzia sinensis*

Based on changes in the distribution area of *Tirpitzia sinensis*, the contraction and expansion of suitable areas during different periods can be compared. Under the SSP126 climate scenario, from 2021 to 2040 compared to the current period, the suitable area of *Tirpitzia sinensis* expanded by 187,547 km² and contracted by 18,922 km². The main expansion regions were southern Shaanxi Province, southern Henan Province, and southern Anhui Province, while the primary contraction region was southwestern Yunnan Province. From 2041 to 2060 compared to 2021–2040, the suitable area expanded by 58,226 km² and contracted by 32,556 km². The main expansion regions were southern Shaanxi Province and southern Gansu Province, while the primary contraction regions were southern Henan Province and central Jiangxi

Province. From 2061 to 2080 compared to 2041–2060, the suitable area expanded by 38,864 km² and contracted by 114,736 km². The main expansion region was southern Henan Province, while the primary contraction regions were central Jiangxi Province and southern Guangdong Province. From 2081 to 2100 compared to 2061–2080, the suitable area expanded by 60,730 km² and contracted by 83,455 km². The main expansion regions were central Sichuan Province and southern Gansu Province, while the primary contraction regions were central Henan Province, central Anhui Province, and southwestern Yunnan Province (Figs. 9 and 10).

Under the SSP585 climate scenario, from 2021 to 2040 compared to the current period, the suitable area of *Tirpitzia sinensis* expanded by 178,944 km² and contracted by 63,675 km². The main expansion zones were southern Henan Province and southern Anhui Province, while the primary contraction zones were southwestern Yunnan Province, central Guangxi Zhuang Autonomous Region, and central Jiangxi Province. From 2041 to 2060 compared to 2021–2040, the suitable area expanded by 185,483 km² and contracted by 77,008 km². The main expansion zones were central Shaanxi Province, central Henan Province, northern Anhui Province, and central Jiangsu Province, while the primary contraction zones were eastern Jiangxi Province, western Fujian Province, and northern Guangdong Province. From 2061 to 2080 compared to 2041–2060, the suitable area expanded by 390,816 km² and contracted by 165,333 km². The main expansion zones were central Shaanxi Province, southern Shanxi Province, northern Henan Province, and southern Shandong Province, while the primary contraction regions were southwestern Yunnan Province, southern Guangdong Province, and central Jiangxi Province. From 2081 to 2100 compared to 2061–2080, the suitable area expanded by 286,700 km² and contracted by 473,088 km². The main expansion zones were southern Gansu Province, northern Shaanxi Province, central Shanxi Province, southwestern Hebei Province, and central-northern Shandong Province, while the primary contraction zones were southwestern Yunnan Province, northern Guangdong Province, eastern Guangxi Zhuang Autonomous Region, eastern Hunan Province, and northwestern Jiangxi Province (Figs. 9 and 10).

Under the current climatic conditions, the distribution center of *Tirpitzia sinensis* is located in Tianzhu County, Qiandongnan Miao and Dong Autonomous Prefecture, Guizhou Province. Under the SSP126 climate scenario, during the periods 2021–2040, 2041–2060, 2061–2080, and 2081–2100, the distribution center is located in Zhijiang Dong Autonomous County, Huaihua City, Hunan Province, with a northwestward shift within Zhijiang Dong Autonomous County. Under the SSP585 climate scenario, the distribution center is located in Zhijiang Dong Autonomous County, Huaihua City, Hunan Province during 2021–2040. In 2041–2060, the center shifts to Mayang Miao Autonomous County, Huaihua City, Hunan Province; in 2061–2080, it moves to Yongshun County, Xiangxi Tujia and Miao Autonomous Prefecture, Hunan Province; and in 2081–2100, it shifts further to Enshi City, Enshi Tujia and Miao Autonomous Prefecture, Hubei Province (Fig. 11). Under the SSP126 climate scenario, the distribution center of *Tirpitzia sinensis* migrates from Guizhou Province to Hunan Province. Under the SSP585 scenario, it migrates from Guizhou Province to Hunan Province and further to Hubei Province. Overall, the distribution center shows a trend of northward migration in the future. Compared to SSP126, the SSP585 climate scenario results in a larger magnitude of distribution center migration.

Discussion

Tirpitzia sinensis, as an important traditional medicinal plant in China, possesses significant medicinal value in its stems and leaves, including promoting blood circulation to remove stasis, reducing swelling and alleviating pain, as well as joining bones and tendons. This study employed the MaxEnt model to predict the potential geographical distribution patterns of this species under current and future climate change scenarios, and identified key environmental factors influencing its distribution, providing a theoretical basis for the scientific conservation and management of this important medicinal plant resource.

Model construction and evaluation

This study systematically integrated 174 distribution point data, covering the core distribution areas in southwestern China and marginal regions in Vietnam. Spatial filtering was performed using ENMtools to effectively reduce data clustering bias. Based on contribution rates and Spearman correlation analysis, 10 key variables (such as bio18 and bio06) were selected from the initial environmental variables, significantly mitigating the risk of overfitting caused by variable collinearity. The Kuenm R package was used to optimize feature combinations (FC) and regularization multipliers (RM), determining the optimal model parameter combination. Model evaluation results showed that after 10 repeated runs, the AUC values for both the training and test sets reached 0.985, indicating excellent predictive performance of the model. However, it should be noted that this study still has the following methodological limitations: First, the issue of spatial autocorrelation has not been fully addressed (Naimi et al., 2011), which may affect the reliability of model parameter estimates; second, independent validation sets or temporally stratified sampling methods were not used for model validation (Hijmans, 2012). These factors may have somewhat impacted the robustness of the model results.

Mechanisms by which key environmental factors influence the distribution of *Tirpitzia sinensis*

The modeling results indicate that the potential geographical distribution of *Tirpitzia sinensis* is primarily influenced by four environmental variables: precipitation of the warmest quarter (bio18), minimum temperature of the coldest month (bio06), standard deviation of temperature seasonality (bio04), and mean temperature of the driest quarter (bio09). These factors collectively constrain the species' distribution limits by affecting water availability, thermal tolerance, and climatic stability, reflecting a multifactorial ecological adaptation strategy.

Among these, bio18 emerged as the most influential variable, with a contribution rate of 57.8%. This variable reflects not only moisture availability during the growing season but also aligns closely with the reproductive phenology of the species. Previous studies have shown that *Tirpitzia sinensis* flowers primarily between May and August (Hu et al., 2021), during which precipitation levels critically influence reproductive success. Excess rainfall during this period can lead to flower drop, thereby reducing fruit set. This sensitivity to summer precipitation partially explains its preference for relatively dry habitats. Such ecological preferences are consistent with its predominant occurrence in limestone karst regions, which are characterized by nutrient-poor soils and rapid water drainage. The minimum temperature of the coldest month (bio06) determines the species' overwintering survival capacity and poses a major constraint on its poleward or altitudinal expansion. Cold stress has been shown to inhibit cell division and compromise membrane integrity, leading to reduced germination and slower growth (Sakai & Larcher, 1987). The suitable temperature range for overwintering in *Tirpitzia sinensis* is estimated to be 2.6–8.1°C, suggesting a limited tolerance to cold environments. Likewise, bio09 plays an important role in regulating the species' physiological activity under seasonal drought. High temperatures during the dry season increase evapotranspiration, and when soil moisture is insufficient, water deficits can result in early wilting and growth suppression (Chaves et al., 2003). Temperature seasonality (bio04), which measures annual temperature fluctuations, also significantly contributes to the model. *Tirpitzia sinensis* tends to inhabit subtropical monsoon regions with relatively stable temperatures, favoring environments with moderate seasonal variability. This likely reflects its need for stable metabolic functioning. Studies have reported that excessive temperature variability can negatively affect seed germination and seedling establishment in shrub species (Jump & Peuelas, 2005), particularly those lacking dormancy mechanisms.

Moreover, the species exhibits morphological adaptations such as thickened leaves and low specific leaf area (SLA), which enhance drought tolerance and water storage capacity. These traits represent a typical resource-conservative strategy, allowing *Tirpitzia sinensis* to survive under water-limited and thermally stressful conditions (Xiong et al., 2022). The synergy between climatic filtering and functional trait expression explains the species' high sensitivity to both temperature and moisture variables, and defines the ecological boundaries of its realized niche.

Impact of future climate change on habitat adaptability of *Tirpitzia sinensis*

Under future climate scenarios, the potential suitable habitat of *Tirpitzia sinensis* is projected to exhibit a general trend of northward expansion. Particularly under the high-emission SSP585 scenario, the total suitable area is expected to reach a peak of 2.344 million km² during the period 2061–2080, with the distribution centroid shifting from Guizhou to parts of Hunan and Hubei. This indicates that *Tirpitzia sinensis* possesses strong climatic niche tracking capacity, enabling it to cope with global warming to some extent through geographic migration toward regions with hot and dry climates.

However, the actual migration process may be constrained by several ecological factors. First, *Tirpitzia sinensis* may exhibit niche conservatism, relying heavily on its native dry-hot environmental conditions and specific soil properties, which could limit its ability to establish in newly suitable regions (Wiens & Graham, 2005). Second, the species primarily relies on insect pollination and short-distance seed dispersal. In the fragmented karst landscape, these dispersal limitations are likely to result in a lagged migration response, with actual expansion rates falling behind the rate of climate-driven habitat shifts (Corlett & Westcott, 2013). In addition, *Tirpitzia sinensis* may face biological interaction challenges in newly suitable areas. Changes in precipitation during the flowering season could interfere with pollinator activity, while native drought-tolerant shrubs may outcompete its seedlings and inhibit population establishment. These factors, which are not accounted for in the current species distribution model, underscore the importance of incorporating ecological processes into future model development for more realistic projections.

It is also worth noting that this study employed a single General Circulation Model (BCC-CSM2-MR) for climate input and did not integrate the uncertainty range derived from multiple climate models (Buisson et al., 2010). Future research should consider CMIP6 multi-model ensemble approaches and dispersal simulations to improve the ecological realism and predictive reliability of habitat shift assessments. In summary, although *Tirpitzia sinensis* demonstrates certain adaptive potential under climate change, the actual shifts in its distribution will be jointly governed by climatic suitability, ecological niche characteristics, species interactions, and dispersal constraints. These insights provide a theoretical basis for climate-resilient conservation and assisted migration strategies for this ecologically specialized medicinal shrub.

Conclusion

This study employed the MaxEnt model with 174 validated distribution records and 10 environmental variables to predict the potential distribution of *Tirpitzia sinensis* in China under current and future climate scenarios. Under current climatic conditions, *Tirpitzia sinensis* is primarily distributed in western Guangxi Zhuang Autonomous Region, southeastern Yunnan Province, southern Guizhou Province, southeastern Sichuan Province, and southwestern Chongqing Municipality. Under future climate change scenarios, the suitable zones for *Tirpitzia sinensis* are expected to expand and exhibit a northward migration trend. In the SSP126 climate scenario, the distribution center of *Tirpitzia sinensis* shifts from Guizhou Province to Hunan Province, while in the SSP585 scenario, it moves further from Guizhou Province to Hunan and Hubei provinces. The main environmental factors influencing the probability of *Tirpitzia sinensis* presence include bio18, bio06, bio04, and bio09. The suitable ranges for these factors are as follows: bio18 (582.4–907.1 mm), bio06 (2.6–8.1°C), bio04 (432.9–712.8), and bio09 (7.7–14.1°C). These findings indicate that *Tirpitzia sinensis* is well-suited to grow in warm and relatively dry regions with adequate precipitation.

Declarations

All authors have read, understood, and have complied as applicable with the statement on “Ethical responsibilities of Authors” as found in the Instructions for Authors.

Conflict of Interest

The research was conducted in the absence of any commercial or financial relationships that could be construed as a potential conflict of interest.

Funding

The author(s) declare financial support was received for the research, authorship, and/or publication of this article. This work was supported by the National Natural Science Foundation of China (32360330, 32360262), China Scholarship Council (202308520101), Guizhou Provincial Program on Commercialization of Scientific and Technological Achievements (QianKeHeChengGuo [2022]010), Water-Fertilizer Coupling and Biodiversity Restoration in Karst Rocky Desertification (QianJiaoJi[2023]004), The Joint Fund of the National Natural Science Foundation of China and the Karst Science Research Center of Guizhou Province (U1812401).

Author Contribution

T.-X.X.and M.-Y.L.conceived and designed the study; M.-Y.L., Z.C., and Z.-R.D. conducted field surveys to obtain partial latitude and longitude data of Tirpitzia sinensis; M.-Y.L. collected the data; T.-X.X. and M.-Y.L. analyzed the data and drafted the manuscript; T.-X.X., M.-Y.L., and S.W. revised various drafts of the manuscript. All authors have read and agreed to the final version of the manuscript.

Acknowledgements

The authors would like to express their sincere gratitude to the WorldClim database for providing the valuable climate data used in this study.

References

1. Bellard, C., Bertelsmeier, C., Leadley, P., Thuiller, W., & Courchamp, F. (2012). Impacts of climate change on the future of biodiversity. *Ecol Lett, 15*(4), 365-377. https://doi.org/10.1111/j.1461-0248.2011.01736.x
2. Bestion, E., Teyssier, A., Richard, M., Clobert, J., & Cote, J. (2015). Live Fast, Die Young: Experimental Evidence of Population Extinction Risk due to Climate Change. *PLoS Biol, 13*(10), e1002281. https://doi.org/10.1371/journal.pbio.1002281
3. Bi, H., Li, X., Guo, M., Liu, X., & Li, J. (2005). Digital Terrain Analysis Based on DEM. *Journal of Beijing Forestry University, 1*(001), 54-58. https://doi.org/10.1007/s11461-005-0002-4
4. Buisson, L., Thuiller, W., Casajus, N., Lek, S., & Grenouillet, G. (2010). Uncertainty in ensemble forecasting of species distribution. *Glob Chang Biol, 16*(4), 1145-1157. https://doi.org/10.1111/j.1365-2486.2009.02000.x
5. Cao, X. (2010). *Prediction of the Potential Suitable Habitats and Risk Assessment of the Alien Invasive Plant Flaveria bidentis in China.*
6. Cao, Y. T., Lu, Z. P., Gao, X. Y., Liu, M. L., Sa, W., Liang, J., . . . Li, Z. H. (2022). Maximum Entropy Modeling the Distribution Area of Morchella Dill. ex Pers. Species in China under Changing Climate. *Biology (Basel), 11*(7). https://doi.org/10.3390/biology11071027

7. Chaves, M. M., Maroco, J. P., & Pereira, J. S. (2003). Understanding plant responses to drought — from genes to the whole plant. *Functional Plant Biology, 30*(3), 239. https://doi.org/10.1071/fp02076
8. Chen, H., Nie, Y., Liu, X., Liu, B., & Zhang, H. (2021). Research on prediction of potential suitable areas of populuseuphratica based on MaxEnt model. *China Agricultural Informatics, 33*(01), 46-55. https://doi.org/10.12105/j.issn.1672-0423.20210105
9. Chen, I. C., Hill, J. K., Ohlemüller, R., Roy, D. B., & Thomas, C. D. (2011). Rapid range shifts of species associated with high levels of climate warming. *Science, 333*(6045), 1024-1026. https://doi.org/10.1126/science.1206432
10. Cobos, M. E., Peterson, A. T., Barve, N., & Osorio-Olvera, L. (2019). kuenm: an R package for detailed development of ecological niche models using Maxent. *PeerJ, 7*, e6281. https://doi.org/10.7717/peerj.6281
11. Corlett, R. T., & Westcott, D. A. (2013). Will plant movements keep up with climate change? *Trends in Ecology & Evolution, 28*(8), 482-488. https://doi.org/10.1016/j.tree.2013.04.003
12. Dillon, M. E., Wang, G., & Huey, R. B. (2010). Global metabolic impacts of recent climate warming. *Nature, 467*(7316), 704-706. https://doi.org/10.1038/nature09407
13. Du, X., Mu, Z., Xiao, Z., Liu, X., Tang, H., & Liu, Z. (2014). Medicinal Plant New Records in Chongqing. *Modern Chinese Medicine, 16*(06), 442-443+450. https://doi.org/10.13313/j.issn.1673-4890.2014.06.003
14. Duan, R. Y., Kong, X. Q., Huang, M. Y., Fan, W. Y., & Wang, Z. G. (2014). The Predictive Performance and Stability of Six Species Distribution Models. *Plos One, 9*. https://doi.org/10.1371/journal.pone.0112764
15. Ehrlén, J., & Morris, W. F. (2015). Predicting changes in the distribution and abundance of species under environmental change. *Ecol Lett, 18*(3), 303-314. https://doi.org/10.1111/ele.12410
16. Fritz, S., See, L., Perger, C., McCallum, I., Schill, C., Schepaschenko, D., . . . Obersteiner, M. (2017). A global dataset of crowdsourced land cover and land use reference data. *Sci Data, 4*, 170075. https://doi.org/10.1038/sdata.2017.75
17. Gao, H., Qian, Q., Liu, L., & Xu, D. (2023). Predicting the Distribution of Sclerodermus sichuanensis (Hymenoptera: Bethylidae) under Climate Change in China. *Insects (2075-4450), 14*(5). https://doi.org/10.3390/insects14050475
18. Gu, R. (2015). *Studies on the Chemical Constituents of Tirpitzia sinensis.* Minzu University of China.
19. Gu, Y., Zhang, F., Liang, X., Liu, C., Xing, S., & Wang, Q. (2020). Integration of natural reserves based on potential habitat protection of the Amur tiger. *Chinese Journal of Ecology, 39*(05), 1590-1599. https://doi.org/10.13292/j.1000-4890.202005.021
20. Hamann, A., & Wang, T. (2006). Potential effects of climate change on ecosystem and tree species distribution in British Columbia. *Ecology, 87*(11), 2773-2786. https://doi.org/10.1890/0012-9658(2006)87[2773:peocco]2.0.co;2

21. Hijmans, R. J. (2012). Cross-validation of species distribution models: removing spatial sorting bias and calibration with a null model. *Ecology, 93*(3). https://doi.org/10.1890/11-0826.1
22. Hu, D., Yao, R., Chen, Y., You, X., Wang, S., Tang, X., & Wang, X. (2021). Tirpitzia sinensis improves pollination accuracy by promoting the compatiblepollen growth. *Biodiversity Science, 29*(07), 887-896.
23. Huang, J., Li, F., Liu, Y., Li, Y., & Tang, X. (2019). Bioinformatic analysis of SSR information in Tirpitzia sinensis transcriptome. *Jiangsu Agricultural Sciences, 47*(02), 54-58. https://doi.org/10.15889/j.issn.1002-1302.2019.02.012
24. Jia, L., Sun, M., He, M., Yang, M., Zhang, M., & Yu, H. (2024). Study on the change of global ecological distribution of Nicotiana tabacum L. based on MaxEnt model. *Frontiers in Plant Science*. https://doi.org/10.3389/fpls.2024.1371998
25. Jump, A. S., & Peuelas, J. (2005). Running to stand still: adaptation and the response of plants to rapid climate change. *Ecol Lett, 8*(9). https://doi.org/10.1111/j.1461-0248.2005.00796.x
26. Li, J., Chen, Y., Guo, Y., He, Y., Fu, J., & Shi, M. (2023). Potential suitable areas of Symphyotrichum subulatum based on MaxEnt under future climate scenarios. *Plant Protection, 49*(02), 92-102. https://doi.org/10.16688/j.zwbh.2022344
27. Li, Y., Tang, X., Wang, L., & Wang, H. (2021). Prediction of Suitable Areas of Fraxinus chinensis in China Under Different Climate Scenarios Based on MaxEnt. *Journal of Northwest Forestry University, 36*(06), 100-107.
28. Liu, H., Guan, L., Huang, G., Cao, J., Yang, H., & Bao, H. (2023). Prediction of Suitable Ecological Distribution Areas for Liriodendron in Hubei Province Using MaxEnt Model. *Hubei Forestry Science and Technology, 52*(02), 9-15.
29. Merilä, J., & Hendry, A. P. (2014). Climate change, adaptation, and phenotypic plasticity: the problem and the evidence. *Evol Appl, 7*(1), 1-14. https://doi.org/10.1111/eva.12137
30. Naimi, B., Skidmore, A. K., Groen, T. A., & Hamm, N. A. S. (2011). Spatial autocorrelation in predictors reduces the impact of positional uncertainty in occurrence data on species distribution modelling. *Journal of Biogeography, 38*(8), 1497-1509. https://doi.org/10.1111/j.1365-2699.2011.02523.x
31. Riahi, K., Vuuren, D. P. V., Kriegler, E., Edmonds, J., O'Neill, B. C., Fujimori, S., . . . Fricko, O. (2017). The Shared Socioeconomic Pathways and their energy, land use, and greenhouse gas emissions implications: An overview. *Global Environmental Change, 42*, 153-168. https://doi.org/10.1016/j.gloenvcha.2016.05.009
32. Sakai, A., & Larcher, W. (1987). Frost survival of plants: responses and adaptation to freezing stress. *Perspective on Politics*. https://doi.org/10.1007/978-3-642-71745-1
33. Thuiller, W., Lavorel, S., Araujo, M. B., Sykes, M. T., & Prentice, I. C. (2005). Climate change threats to plant diversity in Europe. *Proceedings of the National Academy of Sciences, 102*(23), 8245-8250. https://doi.org/10.1073/pnas.0409902102
34. Warren, D. L., Glor, R. E., & Turelli, M. (2010). ENMTools: a toolbox for comparative studies of environmental niche models. *Ecography, 33*. https://doi.org/10.1111/ecog.05485.

35. Wiens, J. J., & Graham, C. H. (2005). Niche Conservatism: Integrating Evolution, Ecology, and Conservation Biology. *Annual Review of Ecology Evolution & Systematics*(1). https://doi.org/10.1146/ANNUREV.ECOLSYS.36.102803.095431
36. Xiong, L., Long, C., Liao, Q., & Xue, F. (2022). Leaf functional traits and their interrelationships with woody plants in karst forest of Maolan. *Chinese Journal of Applied and Environmental Biology, 28*(01), 152-159. https://doi.org/10.19675/j.cnki.1006-687x.2020.09069
37. Zhang, K., Yao, L., Meng, J., & Tao, J. (2018). Maxent modeling for predicting the potential geographical distribution of two peony species under climate change. *Sci Total Environ, 634*, 1326-1334. https://doi.org/10.1016/j.scitotenv.2018.04.112
38. Zhao, G., Cui, X., Wang, Z., jing, H., & Pan, B. (2021). Prediction of Potential Distribution of Ziziphus jujuba var. spinosa in China under Context of Climate Change. *Scientia Silvae Sinicae, 57*(06), 158-168.
39. Zheng, M., Song, Y., Li, C., Na, M., Wu, Y., Ma, J., & Yu, Y. (2024). Analysis of Potential Geographic Distribution of Solanum rostratum Based on Optimized MaxEnt Model in Agro-pastoral Ecotone of Northern China. . *Acta Agrestia Sinica*, 1-14.

Figures

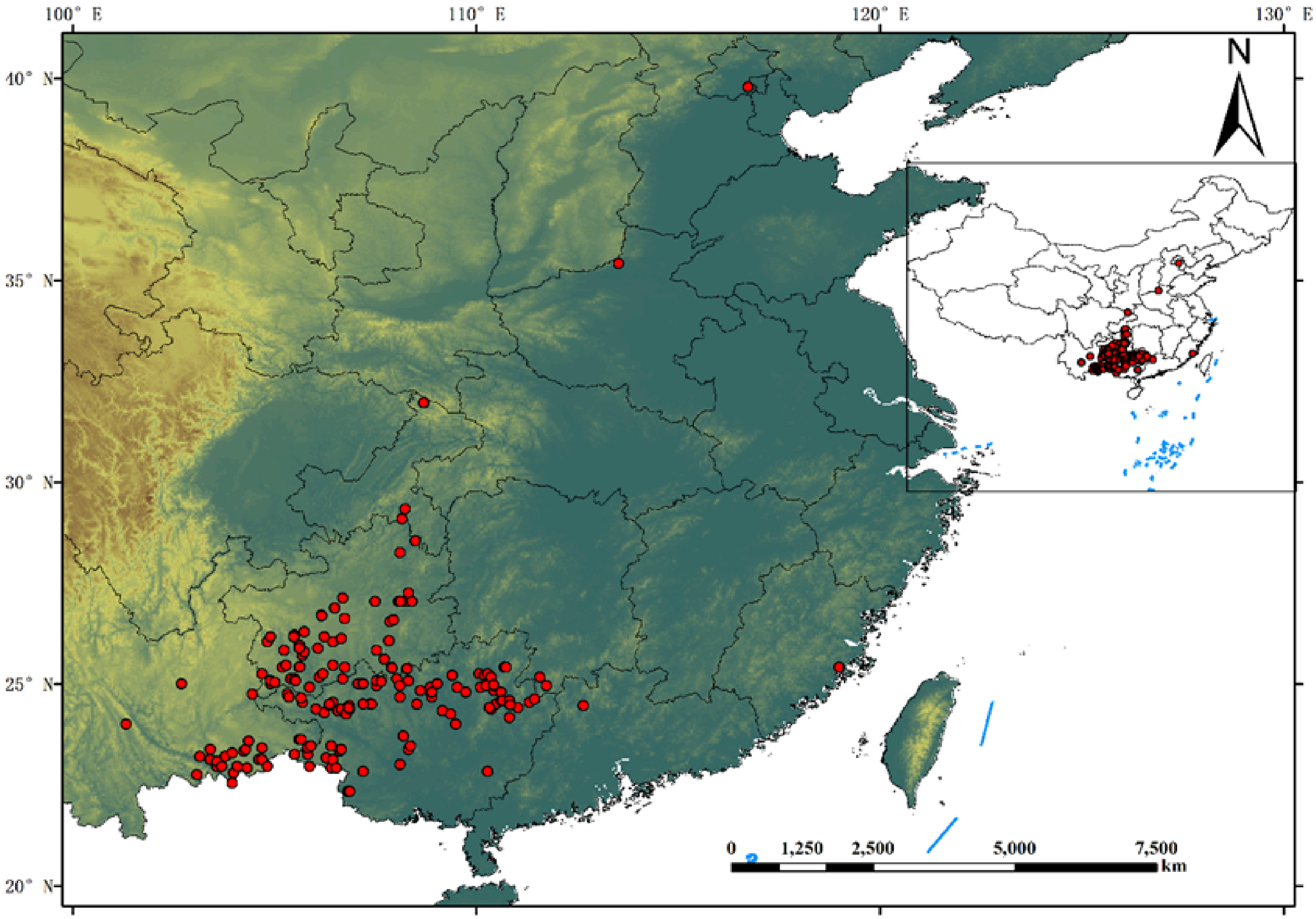

Figure 1

Geographical distribution of *Tirpitzia sinensis* in China

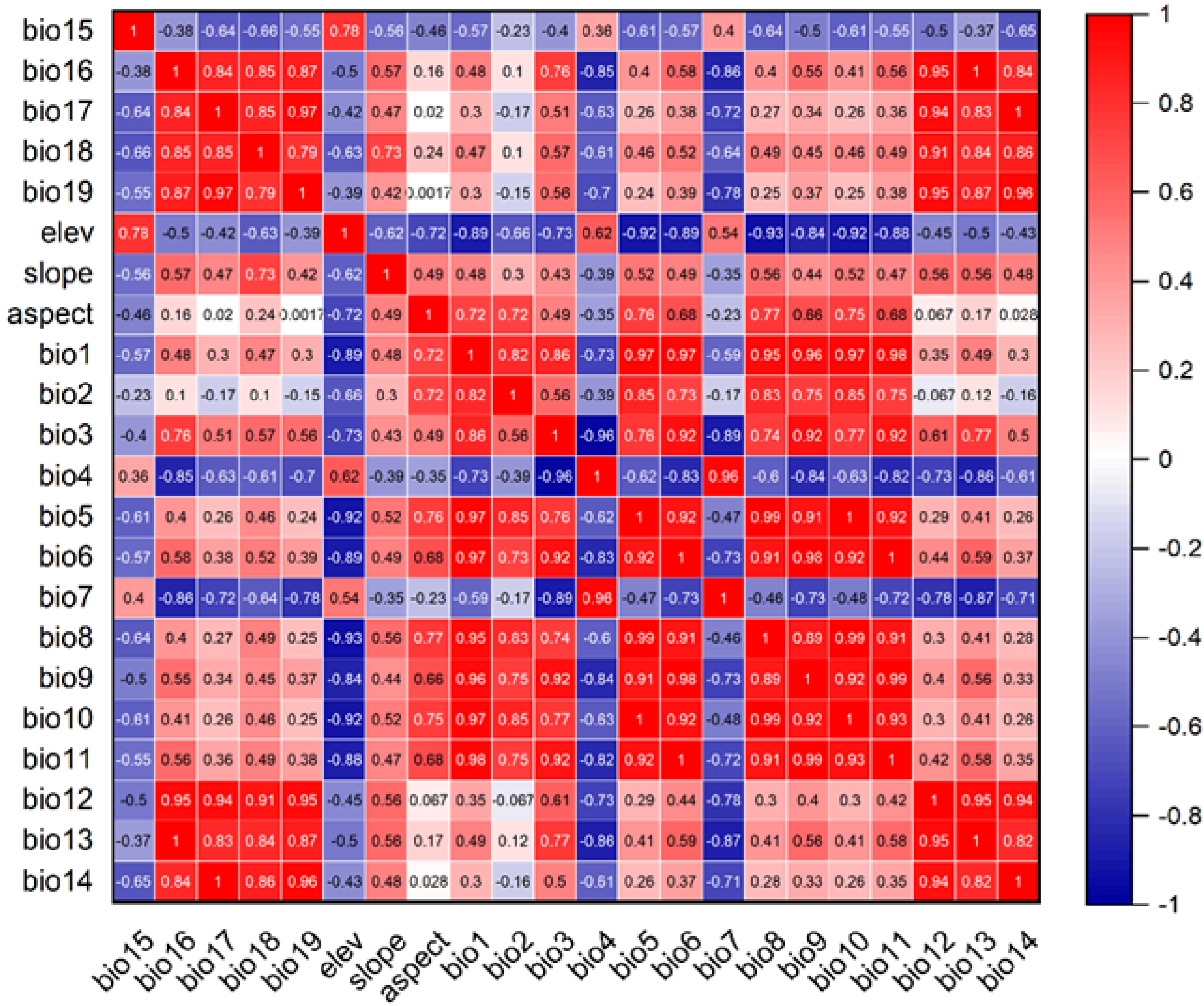

Figure 2

Correlation diagram of 22 environmental variables

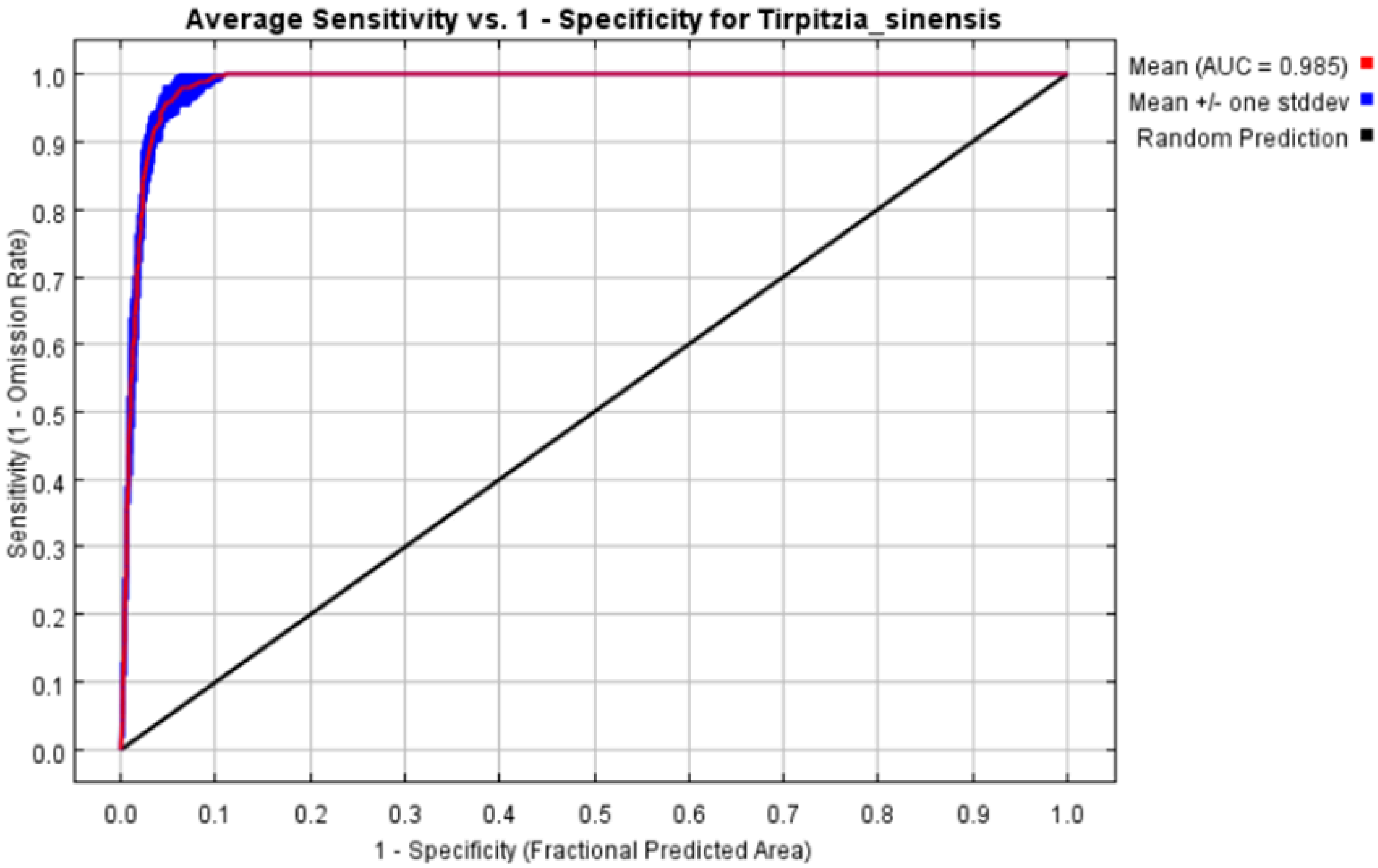

Figure 3

Receiver operating characteristic (ROC) curve of the MaxEnt model

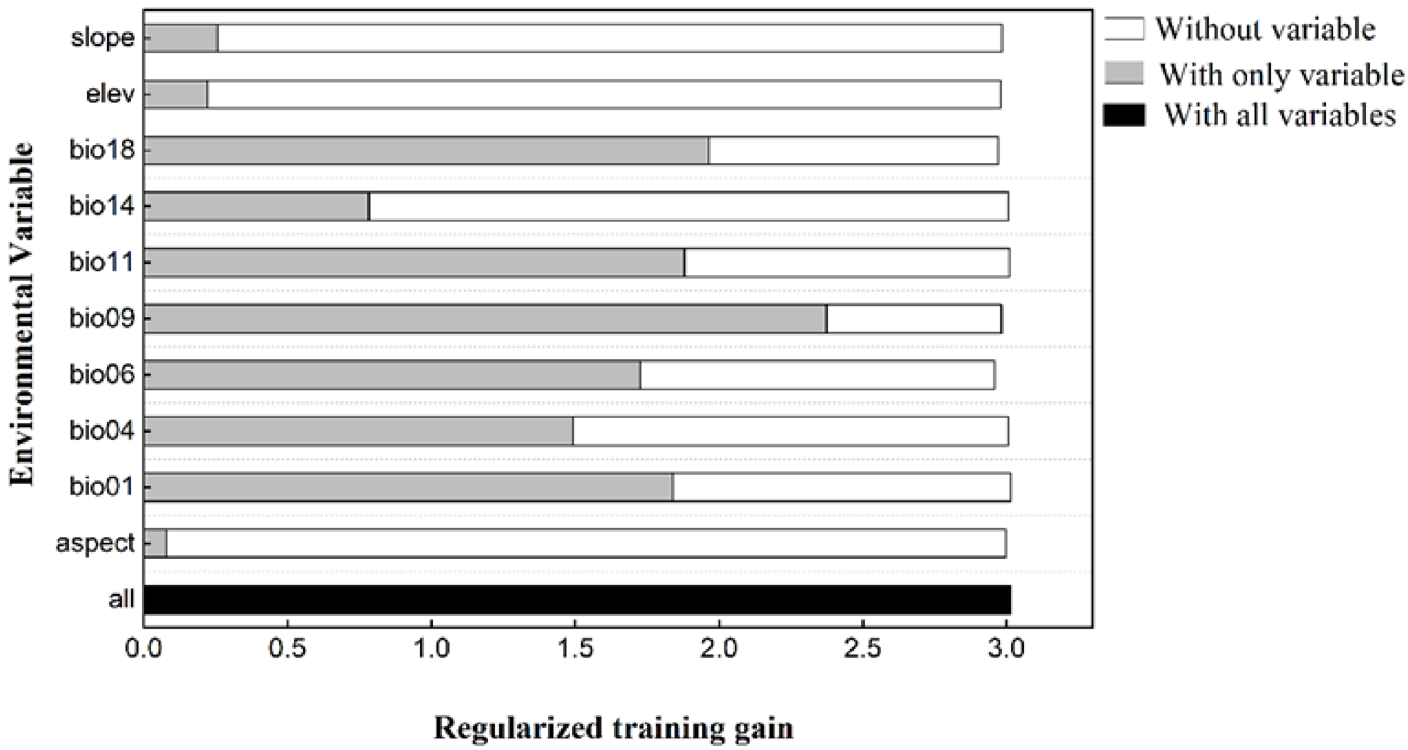

Figure 4

The importance of jackknife analysis of environmental variables

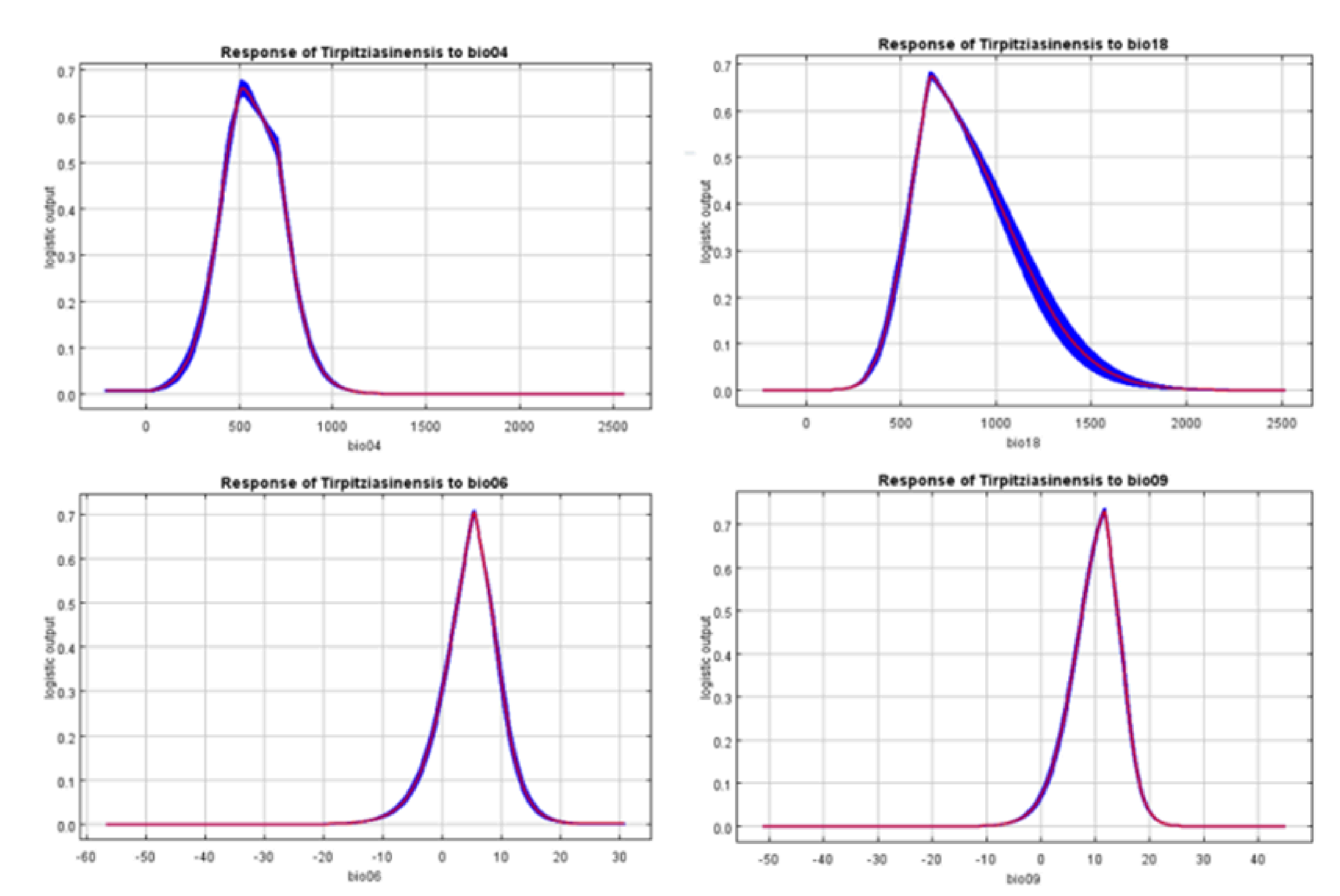

Figure 5

Response curves of probability of presence and environmental factors

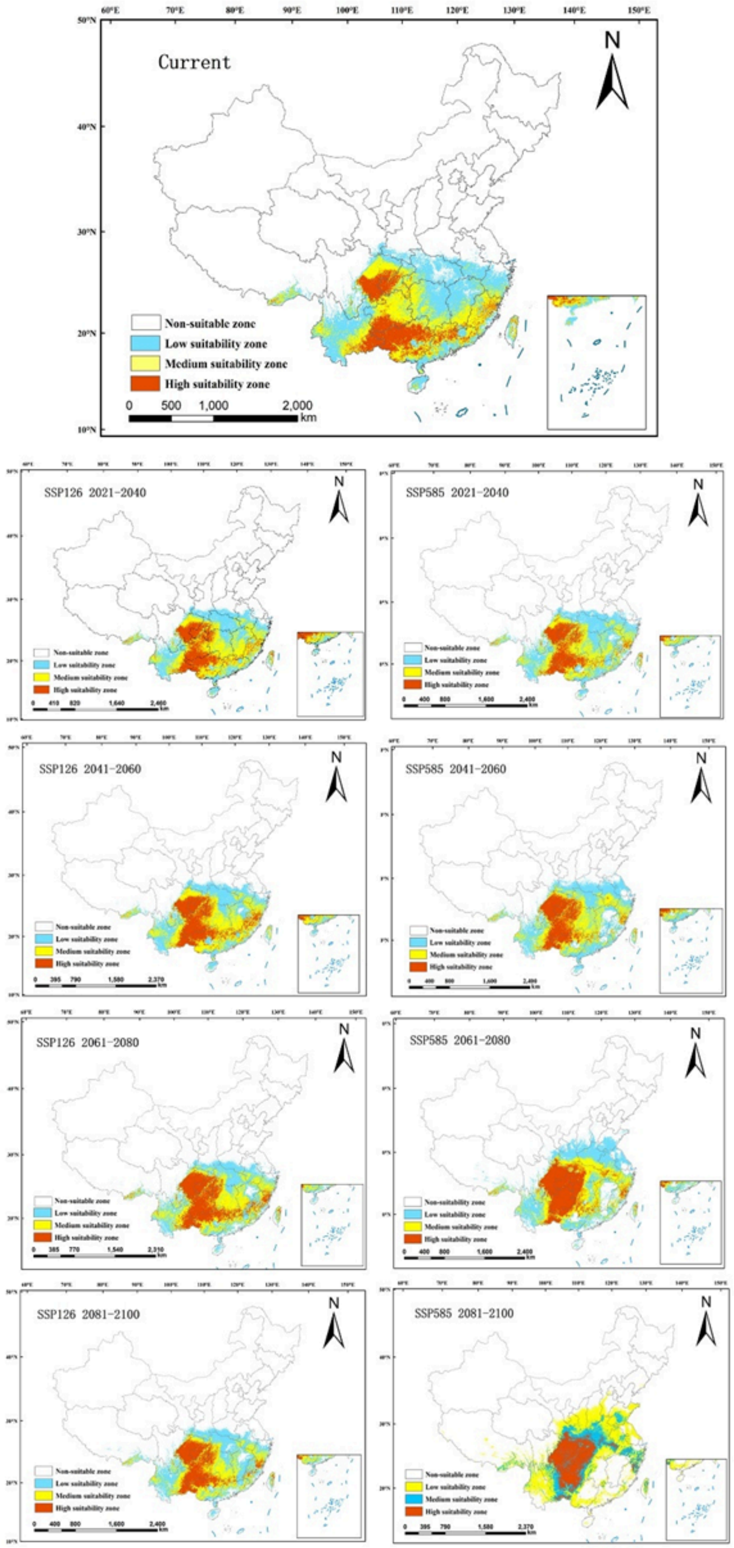

Figure 6

Potential suitable distribution of *Tirpitzia sinensis* in China under different climate scenarios

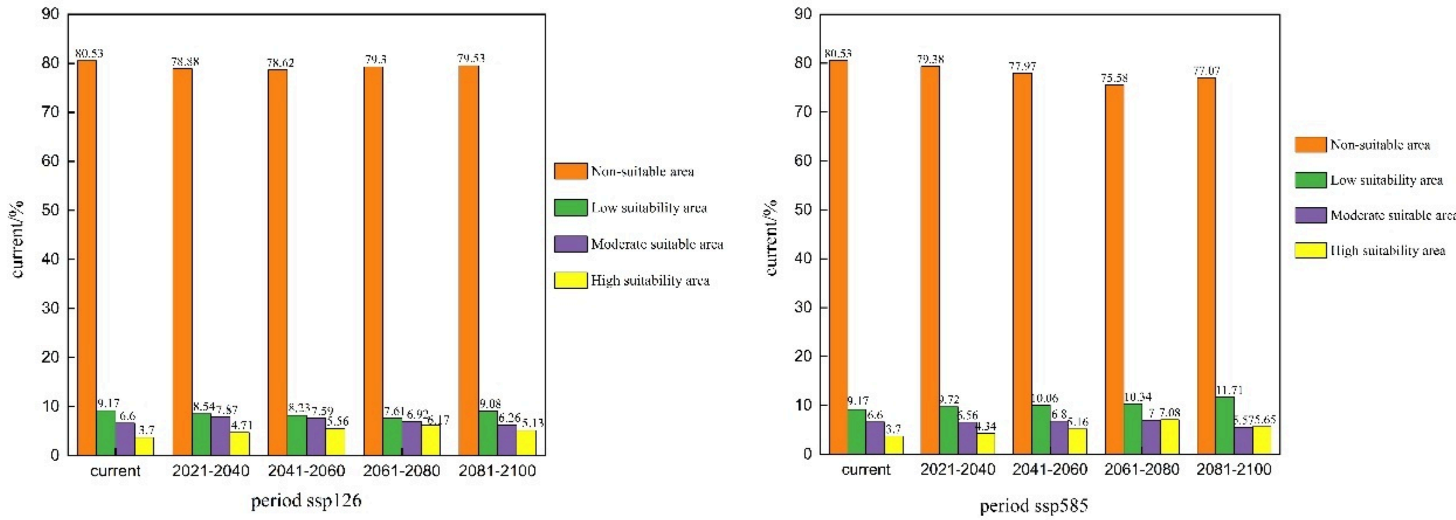

Figure 7

Proportions of habitat suitability ranks for *Tirpitzia sinensis* in China across different time periods

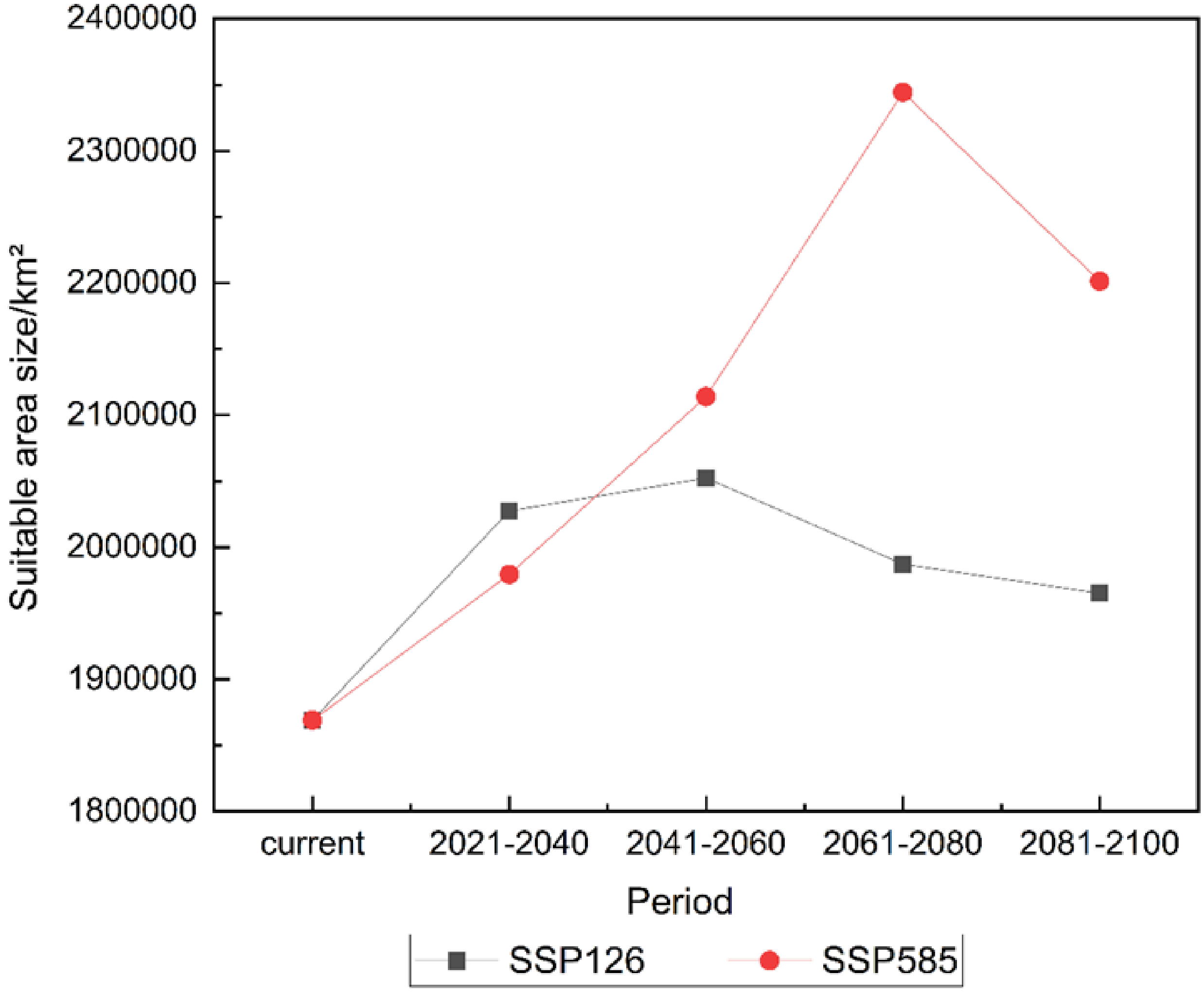

Figure 8

Changes in habitat area for *Tirpitzia sinensis* in China across different time periods

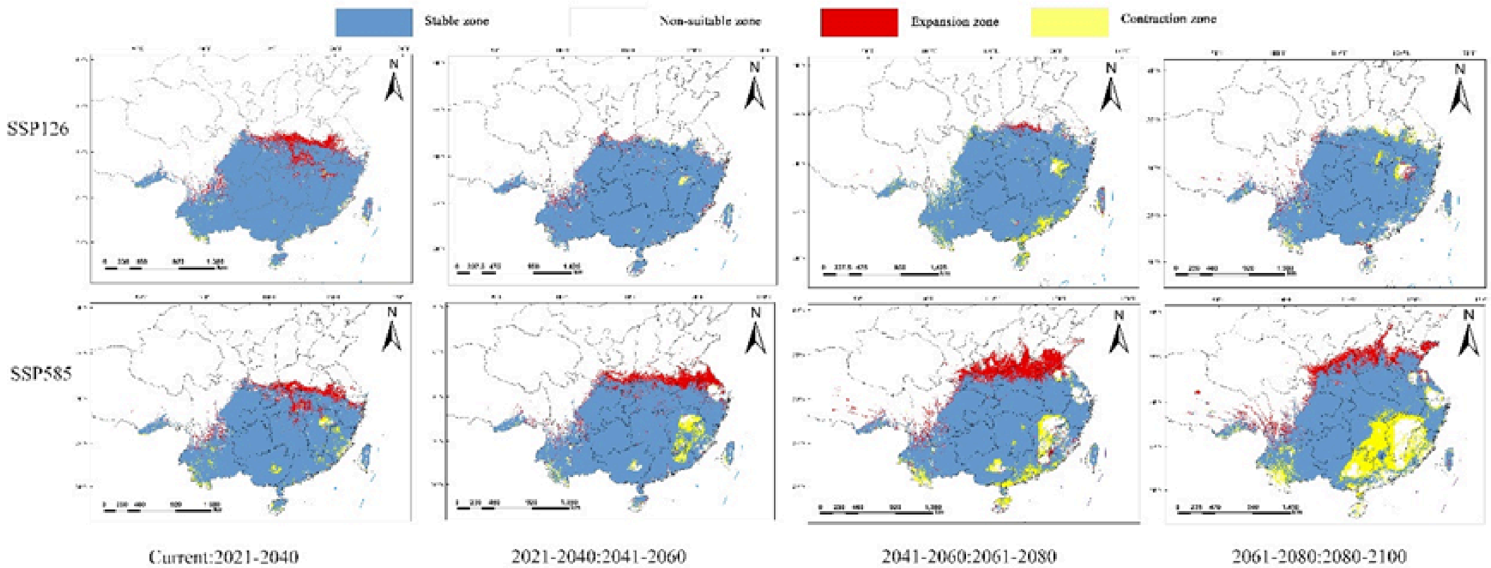

Figure 9

Changes in habitat area of *Tirpitzia sinensis* under different climate scenarios

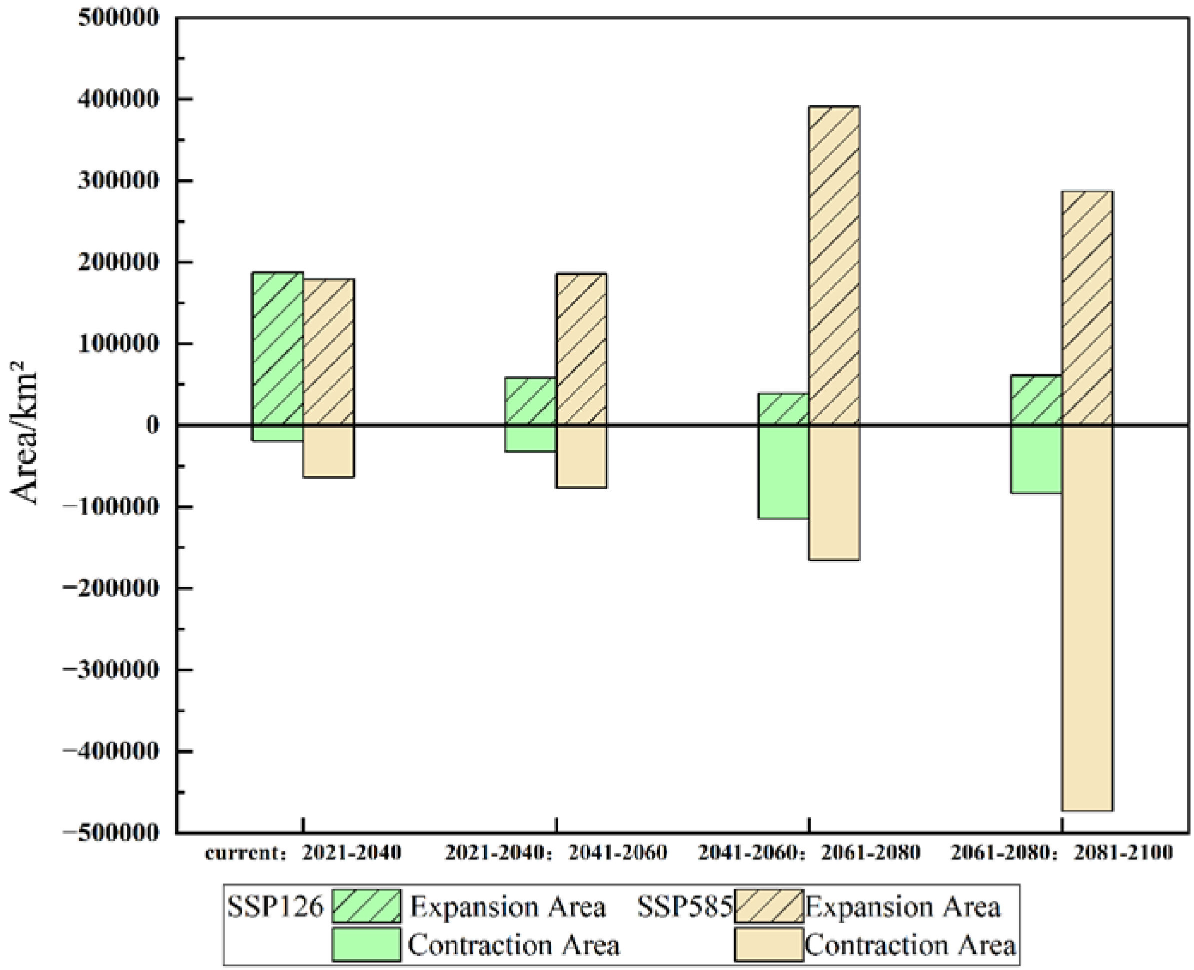

Figure 10

Changes in habitat area of *Tirpitzia sinensis* under two future climate scenarios

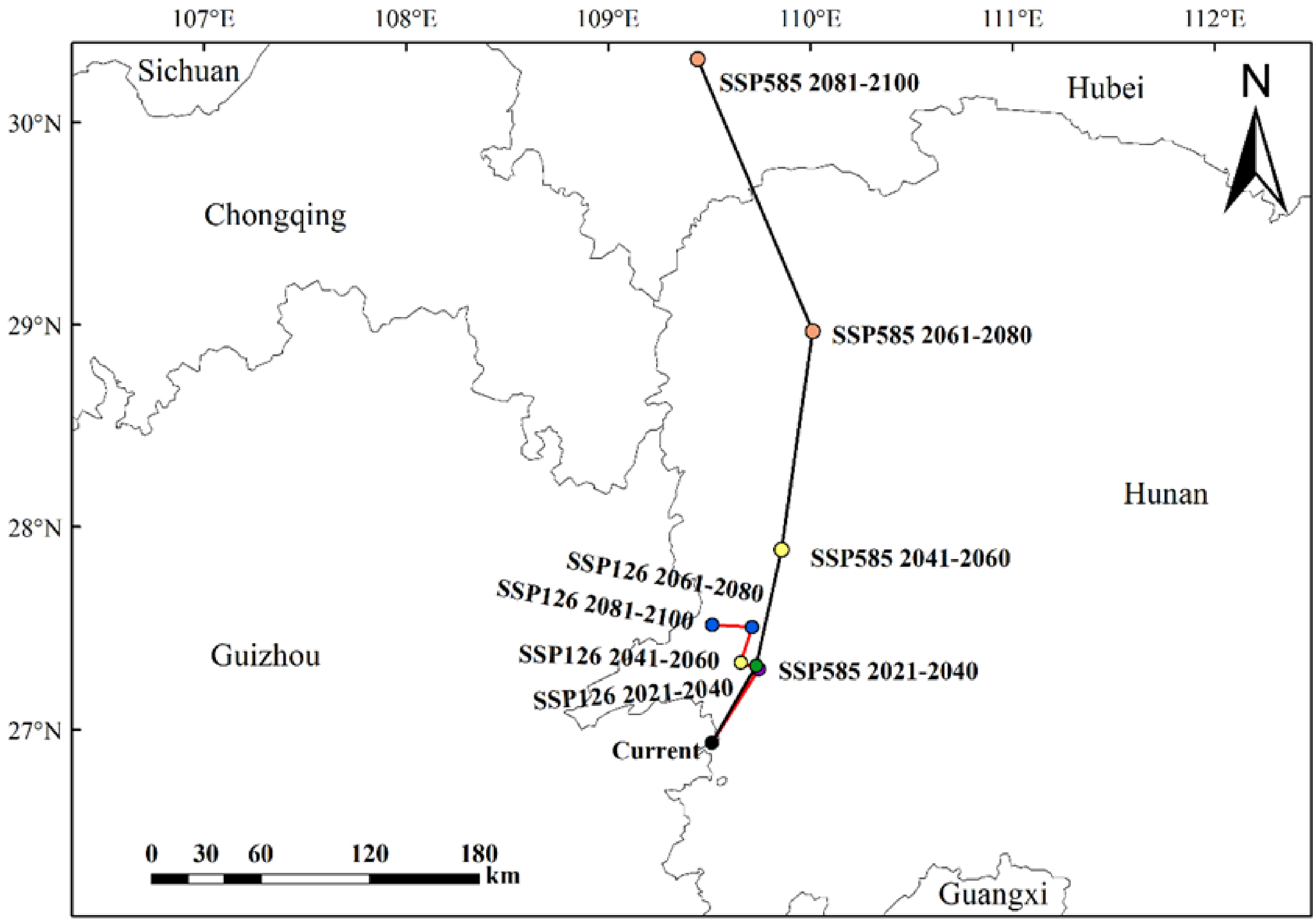

Figure 11

Migration routes of the distribution centroid of *Tirpitzia sinensis* in China under two future climate scenarios